 CMES, vol.56, no.3, pp.303-333, 2010

An Advanced Implicit Meshless Approach for the Non-linear Anomalous Subdiffusion Equation

Y. T. Gu[1], **P. Zhuang**[2] **and F. Liu** [3]

Abstract: Recently, the numerical modelling and simulation for anomalous subdiffusion equation (ASDE), which is a type of fractional partial differential equation(FPDE) and has been found with widely applications in modern engineering and sciences, are attracting more and more attentions. The current dominant numerical method for modelling ASDE is Finite Difference Method (FDM), which is based on a pre-defined grid leading to inherited issues or shortcomings. This paper aims to develop an implicit meshless approach based on the radial basis functions (RBF) for numerical simulation of the non-linear ASDE. The discrete system of equations is obtained by using the meshless shape functions and the strong-forms. The stability and convergence of this meshless approach are then discussed and theoretically proven. Several numerical examples with different problem domains are used to validate and investigate accuracy and efficiency of the newly developed meshless formulation. The results obtained by the meshless formulations are also compared with those obtained by FDM in terms of their accuracy and efficiency. It is concluded that the present meshless formulation is very effective for the modelling and simulation of the ASDE. Therefore, the meshless technique should have good potential in development of a robust simulation tool for problems in engineering and science which are governed by the various types of fractional differential equations.

Keywords: anomalous subdiffusion equation, fractional differential equation, numerical simulation, meshless method, radial basis functions

[1] School of Engineering Systems, Queensland University of Technology, G. P. O. Box 2434, Brisbane, QLD 4001, Australia

[2] School of Mathematical Sciences, Xiamen University, Xiamen, 361005, China.

[3] School of Mathematical Sciences, Queensland University of Technology, G. P. O. Box 2434, Brisbane, QLD 4001, Australia

1 Introduction

Recently, because of the new developments in advanced bio-engineering, sustainable environment and renewable energy, which are often governed by a series of fractional ordinary differential equations (FODE) [Ye and Ding (2009); Kou, Yan, and Liu (2009)] or fractional partial differential equations (FPDE) [Sokolov and Klafter (2005); Benson, Wheatcraft, and Meerschaert (2000)], the numerical simulation of FPDE is becoming important. It has been reported that, in numerous physical and biological systems, many diffusion rates of species cannot be characterized by the single parameter of the diffusion constant [Sokolov and Klafter (2005)]. Instead, the (anomalous) diffusion is characterized by a scaling parameter α as well as a diffusion constant K, and the mean square displacement of diffusing species $\langle x^2(t)\rangle$ scales as a nonlinear power-law in time, i.e.,

$$\langle x^2(t)\rangle \sim \frac{2K_\alpha}{\Gamma(1+\alpha)}t^\alpha, \ \ t\to\infty,$$

where α $(0<\alpha<1)$ is the anomalous diffusion exponent and K_α is the generalized diffusion coefficient. Ordinary (or Brownian) diffusion corresponds to $\alpha=1$ with $K_1=D$ (the ordinary diffusion coefficient). For example, single particle tracking experiments and photo-bleaching recovery experiments have revealed subdiffusion $(0<\alpha<1)$ of proteins and lipids in a variety of cell membranes [Brown, Wu, Zipfel, and Webb (1999); Feder, Brust-Mascher, Slattery, Baird, and Webb (1996); Ghosh (1991); Ghosh and Webb (1994); Sheets, Lee, Simson, and Jacobson (1997); Slattery (1991); Smith, Morrison, Wilson, Fernandez, and Cherry (1999)]. Anomalous subdiffusion has also been observed in neural cell adhesion molecules [Simson, Yang, Moore, Doherty, Walsh, and Jacobson (1998)]. Indeed anomalous subdiffusion (the case with $0<\alpha<1$) is generic in media with obstacles [Saxton (1994, 2001)] or binding sites [Saxton (1996)]. For anomalous subdiffusive random walks, the continuum description via the ordinary diffusion equation is replaced by the anomalous subdiffusion equations. The numerical modelling and simulation for the anomalous subdiffusion equations are attracting more and more attentions from researchers [Agrawal, Machado, and Sabatier (2004), Butzer and Georges (2000), Kenneth and Bertram (1993), Yuste and Acedo (2005), Langlands and Henry (2005), Chen, Liu, Turner, and Anh (2007), Zhuang, Liu, Anh, and Turner (2008)]. Fractional kinetic equations (FKE) including a class of anomalous subdiffusion equations, such as fractional diffusion equation, modified anomalous subdiffusion equation, fractional advection-diffusion equation, fractional Fokker-Planck equation, fractional cable equation etc., are recognized as useful approaches for the description of transport dynamics in complex systems including systems exhibiting Halmiltonian chaos, disordered medium, plasma and fluid turbulence,

underground water pollution, dynamics of protein molecules, motions under the influence of optical tweezers, reactions in complex systems, and more [Chechkin, Gonchar, Kflafter, and Metzler (2006), Metzler and Klafter (2000), Metzler and Klafter (2004), Sokolov, Klafter, and Blumen (2002), Zaslavsky (2002)]. When the fractional kinetic equations describe the asymptotic behaviour of continuous time random walks, their solutions correspond to the Lévy walks. The advantage of the fractional kinetic model basically lies in the straightforward way of including external force terms and of calculating boundary value problems. Therefore, FKE results in a more accurate representation of the relative phenomena than normal partial differential equations (PDE). Unlike the normal PDE, the differential order (regarding to time or space or both) of a FKE is not with a integer order, in other words, the differential order might be a fractional order (i.e., 0.5th order, 1.5th order, and so on), which will lead to a big difficulty in numerical simulation, because most existing numerical simulation techniques are developed for the PDE with a integer differential order.

Yuste and Acedo [Yuste and Acedo (2005)] proposed an explicit Finite Difference Method(FDM) and a new Von Neumann-type stability analysis for the anomalous subdiffusion equation. However, they did not give a convergence analysis and pointed out the difficulty of this task when implicit methods was used. Implicit difference method is usually unconditional stable and convergent, but the explicit difference method is different. Langlands and Henry [Langlands and Henry (2005)] proposed an implicit numerical scheme (L_1 approximation) to analyze this problem, and discussed the accuracy and stability of this scheme. However, they did not derive the global accuracy of this implicit numerical scheme and failed in establishing the unconditional stability for all γ in the range $0 < \gamma \leq 1$. Chen and Liu et al. [Chen, Liu, Turner, and Anh (2007)] presented a Fourier method for the anomalous subdiffusion equation, and they analyzed the stability and the global accuracy of the difference approximation scheme. Zhuang and Liu et al. [Zhuang, Liu, Anh, and Turner (2008)] also proposed analytical techniques of implicit numerical methods for the anomalous subdiffusion equation. At present, most of the anomalous subdiffusion equations were solved numerically by Finite Difference Method (FDM) in one dimensional case [Langlands and Henry (2005); Yuste and Acedo (2005); Chen, Liu, Turner, and Anh (2007); Zhuang, Liu, Anh, and Turner (2008)], and a few research has been reported using Finite Element Method (FEM) for this problem [Ervin and Roop (2005); Ervin, Heuer, and Roop (2007)].

FDM and FEM are numerical approaches based on pre-defined meshes/grids, which lead to inherited issues or shortcomings including: a) difficulty in handling a complicated problem domain; b) difficulty in handling the Newman boundary conditions, c) difficulty in handling irregular nodal distribution; d) difficulty in conduct-

ing adaptive analysis, and e) low accuracy. Therefore, these shortcomings become the main barrier for the development of a powerful simulation tool for real applications governed by FPDE. In addition, most current research in this field is still limited in some one-dimensional (1-D) or two-dimensional (2-D) benchmark problems with very simple problem domains (i.e., squares and rectangles) and Dirichletle boundary conditions. It already becomes crucial to develop an alternative numerical technique for modeling and simulation of FPDE.

Recent years, a group of meshless (or meshfree) methods have been developed and successfully used in many fields. Depending on whether a numerical integration is used in developing the system of algebraic equations, the meshless methods can be largely grouped into two different categories: meshless methods based on collocation techniques (with Dirac-delta-test functions) and meshless methods based on the general weak-forms (with non-Dirac-delta-test function) of ordinary (partial) differential equations (ODEs or PDEs). The meshless methods based on collocation techniques have a relatively long history, and they include smooth particle hydrodynamics (SPH) [Gingold and Moraghan (1977)], the meshless collocation methods [Kansa (1990); Le, Mai-Duy, Tran-Cong, and Baker (2008)], finite point method (FPM) [Onate, Idelsohn, Zienkiewicz, Taylor, and Sacco (1996)], etc. The so-called meshless methods, using various global weak-forms, were proposed about twenty years ago. This category of meshless methods includes the diffuse element method (DEM) [Nayroles, Touzot, and Villon (1992)], the element-free Galerkin (EFG) method [Belytschko, Lu, and Gu (1994)], and so on. The meshless methods based on the weak-forms, in general, exhibit very good stability and accuracy. Therefore, they have been successfully applied in problems of solid mechanics and fluid mechanics. However, in particular, the above-mentioned so-called meshless methods are meshless only in terms of the interpolation of the field variables, as compared to the conventional FEM. Most of them have to use global background cells (mesh) to integrate a weak-form over a global problem domain. The global background mesh for integration makes them to be not truly meshless, or they can be considered as advanced or modified cases of the FEM. In order to alleviate the global integration background mesh, the meshless local Petrov-Galerkin (MLPG) methods were proposed by Atluri et al. [Atluri and Zhu (1998a); Atluri and Zhu (1998b); Atluri, Kim, and Cho (1999); Atluri and Shen (2002a);Atluri and Shen (2002b); Atluri, Han, and Rajendran (2004); Li and Atluri (2008); Gu and Liu (2001); Ching and Batra (2001); Zheng, Long, Xiong, and Li (2009)]. In the MLPG, Petorv-Galerkin local weak-forms, integrated in regular-shaped local domains, were developed. The local integration domain can be as simple as possible (such as circles, ellipses, rectangles, or triangles in 2-D; spheres, rectangular parallelepipeds, or ellipsoids in 3-D) and can be automatically constructed in com-

puting. Therefore, MLPG advances a big step to the final target of a truly meshless method.

The above discussed meshless methods have demonstrated some distinguished advantages [Liu and Gu (2005)] including: 1) they do not use a mesh (at least in field approximation), so that the burden of mesh generation in FDM and FEM is overcome. Hence, an adaptive analysis is also easily achievable; 2)they are usually more accurate than FDM and FEM due to the use of higher order meshless trial functions; and 3)they are capable of solving complex problems that are difficult for the conventional FDM and FEM. Because of these unique advantages, meshless methods seem to have a good potential for the simulation of FSDE. Although the meshless methods have been successfully applied to a wide range of problems, for which, however, the governing equations are conventional PDE with an integer order, very limited work was reported to handle fractional partial differential equations (FPDE) by the meshless techniques [Chen, Ye, and Sun (2010)]. This topic calls for a significant development.

The objective of this paper is to develop an implicit meshless formulation based on the radial basis functions (RBF) for numerical simulation of non-linear anomalous subdiffusion equation(ASDE). The discrete equations for two-dimensional non-linear ASDE are obtained, based on the meshless shape functions and the strong-forms. The essential boundary conditions are enforced by the direct collocation method [Zhu and Atluri (1998); Atluri, Kim, and Cho (1999)]. The stability and convergence of this method are then discussed and theoretically proven. Several numerical examples with different problem domains and different nodal distributions are used to validate and investigate accuracy and efficiency of the newly developed meshless formulation.

The paper is organized as follows: a finite difference scheme for temporal discretization of time is proposed in Section 2, where the stability and convergence analysis is given. The RBF interpolation approximation is briefed in Section 3. In Section 4, we propose the meshless scheme for temporal discretization. Numerical examples are studied and discussed in Section 5. Finally, conclusions are presented in Section 6.

2 Discretization of time

Subdiffusive motion is particularly important in the context of complex systems such as glassy and disordered materials, in which pathways are constrained for geometric or energetic reasons. For anomalous subdiffusive random walkers, the continuum description via the ordinary diffusion equation is replaced by the fractional diffusion equation[Metzler and Klafter (2000), Yuste and Acedo (2004), Yuste and

Acedo (2005), Langlands and Henry (2005)].

In this paper, we consider the following anomalous subdiffusion equation with nonlinear source term

$$\frac{\partial u(\mathbf{x},t)}{\partial t} = \kappa_0 D_t^{1-\alpha}\left[\Delta u(\mathbf{x},t)\right] + f(u,\mathbf{x},t),\ \ x \in \Omega \subset \mathbf{R}^d,\ \ t>0 \tag{1}$$

together with the general boundary and initial conditions

$$u(\mathbf{x},t) = g(\mathbf{x},t),\ \ \mathbf{x} \in \partial\Omega \subset \mathbf{R}^d,\ \ 0<t\le T \tag{2}$$

$$u(\mathbf{x},t) = u_0(\mathbf{x}),\ \ t=0 \tag{3}$$

where Δ is the Laplace differential operator, Ω is a bounded domain in $\mathbf{R}^d$, $\partial\Omega$ is the boundary of Ω, κ the diffusion coefficient, $f(u,\mathbf{x},t)$, $g(\mathbf{x},t)$ and $u_0(\mathbf{x})$ are known functions. We suppose that the function $f(u,\mathbf{x},t)$ satisfies the Lipschitz condition, i.e.,

$$|f(u_1,\mathbf{x},t) - f(u_2,\mathbf{x},t)| \le L|u_1-u_2|,\ \ \forall u_1,u_2. \tag{4}$$

In Eq. (1), ${}_0D_t^{1-\alpha}u(\mathbf{x},t)$ is the Riemann-Liouville fractional derivative of order $1-\alpha$ $(0<\alpha<1)$ defined as

$${}_0D_t^{1-\alpha}u(\mathbf{x},t) = \frac{1}{\Gamma(\alpha)}\frac{\partial}{\partial t}\int_0^t (t-\eta)^{\alpha-1}u(\mathbf{x},\eta)d\eta. \tag{5}$$

2.1 Time Discretization

Define $t_k = k\Delta t,\ \ k=0,1,2,\ldots,K$, where $\Delta t = T/K$ is time stepsize. And we suppose that $\Delta t \le 2/(3L)$.

By integrating both sides of (1), we obtain

$$u(\mathbf{x},t_{k+1}) - u(\mathbf{x},t_k) = \kappa\left[{}_0D_t^{-\alpha}\Delta u(\mathbf{x},t_{k+1}) - {}_0D_t^{-\alpha}\Delta u(\mathbf{x},t_k)\right] + \int_{t_k}^{t_{k+1}} f(u,\mathbf{x},t)dt \tag{6}$$

where the time fractional integral ${}_0D_t^{-\alpha}u(\mathbf{x},t_k)$ at $t=t_k$ can be approximated as follow

$$\begin{aligned} {}_0D_t^{-\alpha}u(\mathbf{x},t_k) &= \tfrac{1}{\Gamma(\alpha)}\sum_{j=0}^{k-1}\int_{t_j}^{t_{j+1}}(t_k-\eta)^{\alpha-1}u(\mathbf{x},\eta)d\eta \\ &= \tfrac{1}{\Gamma(\alpha)}\sum_{j=0}^{k-1}u(\mathbf{x},t_{j+1})\int_{t_j}^{t_{j+1}}(t_k-\eta)^{\alpha-1}d\eta + \widetilde{R}_k \end{aligned} \tag{7}$$

where

$$\begin{aligned}\widetilde{R}_k &= \tfrac{1}{\Gamma(\alpha)}\sum_{j=0}^{k-1}\int_{t_j}^{t_{j+1}}[u(\mathbf{x},\eta)-u(\mathbf{x},t_{j+1})]\cdot(t_k-\eta)^{\alpha-1}d\eta \\ &= \tfrac{1}{\Gamma(\alpha)}\sum_{j=0}^{k-1}\left[u(\mathbf{x},\xi_1^{(j)})-u(\mathbf{x},t_{j+1})\right]\int_{t_j}^{t_{j+1}}(t_k-\eta)^{\alpha-1}d\eta \\ &= \tfrac{1}{\Gamma(\alpha)}\sum_{j=0}^{k-1}\tfrac{\partial u(\mathbf{x},\xi_2^{(j)})}{\partial t}(\xi_1^{(j)}-t_j)\int_{t_j}^{t_{j+1}}(t_k-\eta)^{\alpha-1}d\eta\end{aligned}$$

and $t_j \le \xi_1^{(j)} \le \xi_2^{(j)} \le t_{j+1}$.
Suppose that $\frac{\partial u(\mathbf{x},t)}{\partial t} \in C(\Omega\times[0,T])$, then

$$|\widetilde{R}_k| \le \frac{Ct_k^{\alpha}}{\Gamma(1+\alpha)}\Delta t \max_{\mathbf{x}\in\Omega,t\in[0,T]}\left|\frac{\partial u(\mathbf{x},t)}{\partial t}\right|. \tag{8}$$

Let $b_j=(j+1)^{\alpha}-j^{\alpha}$, $j=0,1,2,\ldots,K$, then Eq. (7) can be rewritten as

$${}_0D_t^{-\alpha}u(\mathbf{x},t_k) = \frac{(\Delta t)^{\alpha}}{\Gamma(1+\alpha)}\sum_{j=0}^{k-1}b_{k-1-j}u(\mathbf{x},t_{j+1})+\widetilde{R}_k, \tag{9}$$

or

$${}_0D_t^{-\alpha}u(\mathbf{x},t_k) = \tfrac{(\Delta t)^{\alpha}}{\Gamma(1+\alpha)}\sum_{j=0}^{k-1}b_j u(\mathbf{x},t_{k-j})+\widetilde{R}_k. \tag{10}$$

Because

$$\begin{aligned}&{}_0D_t^{-\alpha}u(\mathbf{x},t_{k+1}) \\ &= \tfrac{1}{\Gamma(\alpha)}\textstyle\int_0^{t_{k+1}}(t_{k+1}-\eta)^{\alpha-1}u(\mathbf{x},\eta)d\eta \\ &= \tfrac{1}{\Gamma(\alpha)}\textstyle\int_0^{\Delta t}(t_{k+1}-\eta)^{\alpha-1}u(\mathbf{x},\eta)d\eta+\tfrac{1}{\Gamma(\alpha)}\int_{t_1}^{t_{k+1}}(t_{k+1}-\eta)^{\alpha-1}u(\mathbf{x},\eta)d\eta \\ &= \tfrac{1}{\Gamma(\alpha)}\textstyle\int_0^{\Delta t}(t_{k+1}-\eta)^{\alpha-1}u(\mathbf{x},\eta)d\eta+\tfrac{1}{\Gamma(\alpha)}\int_0^{t_k}(t_k-\eta)^{\alpha-1}u(\mathbf{x},\eta+\Delta t)d\eta,\end{aligned}$$

thus,

$$\begin{aligned}&{}_0D_t^{-\alpha}u(\mathbf{x},t_{k+1})-{}_0D_t^{-\alpha}u(\mathbf{x},t_k) \\ &= \tfrac{1}{\Gamma(\alpha)}\textstyle\int_0^{\Delta t}(t_{k+1}-\eta)^{\alpha-1}u(\mathbf{x},\eta)d\eta \\ &+\tfrac{1}{\Gamma(\alpha)}\textstyle\int_0^{t_k}(t_k-\eta)^{\alpha-1}[u(\mathbf{x},\eta+\Delta t)-u(\mathbf{x},\eta)]\,d\eta,\end{aligned}$$

From (10) and (8), we have[Zhuang, Liu, Anh, and Turner (2008)]

$$\begin{aligned}&\tfrac{1}{\Gamma(\alpha)}\textstyle\int_0^{t_k}(t_k-\eta)^{\alpha-1}[u(\mathbf{x},\eta+\Delta t)-u(\mathbf{x},\eta)]\,d\eta \\ &= \tfrac{(\Delta t)^{\alpha}}{\Gamma(1+\alpha)}\textstyle\sum_{j=0}^{k-1}b_j\left[u(\mathbf{x},t_{k+1-j})-u(\mathbf{x},t_{k-j})\right]+R_k^{(1)},\end{aligned}$$

where

$$|R_k^{(1)}| \leq \frac{Ct_k^{\alpha}}{\Gamma(1+\alpha)}\Delta t \max_{\mathbf{x}\in\Omega,t>0}\left|\frac{\partial\left[u(\mathbf{x},t+\Delta t)-u(\mathbf{x},t)\right]}{\partial t}\right| \leq C_1(\Delta t)^2.$$

Note that[Zhuang, Liu, Anh, and Turner (2008)]

$$\begin{aligned}\tfrac{1}{\Gamma(\alpha)}\int_0^{\Delta t}(t_{k+1}-\eta)^{\alpha-1}u(\mathbf{x},\eta)d\eta &= \tfrac{1}{\Gamma(\alpha)}\int_0^{\Delta t}(t_{k+1}-\eta)^{\alpha-1}u(\mathbf{x},\Delta t)d\eta + R_k^{(2)}\\ &= \tfrac{b_k}{\Gamma(1+\alpha)}u(\mathbf{x},t_1)+R_k^{(2)},\end{aligned}$$

where $|R_k^{(2)}| \leq C_2 b_k(\Delta t)^{1+\alpha}$.

We also have

$$\int_{t_k}^{t_{k+1}} f(u,\mathbf{x},\eta)d\eta = \frac{\Delta t}{2}\left[f(u(\mathbf{x},t_{k+1}),\mathbf{x},t_{k+1})+f(u(\mathbf{x},t_k),\mathbf{x},t_k)\right]+R_k^{(3)},$$

where $|R_k^{(3)}| \leq C_3(\Delta t)^2$.

Lemma 1[Zhuang, Liu, Anh, and Turner (2008)] The coefficients $b_k(k=0,1,2\ldots,K)$ satisfy

(1)$b_0 = 1 > b_1 > b_2 > \ldots > b_K > 0$,

(2)There is a positive constant $C>0$ such that $\Delta t \leq Cb_k(\Delta t)^{\alpha}$.

Thus, from (6) we can obtain

$$\begin{aligned}u(\mathbf{x},t_{k+1}) &= u(\mathbf{x},t_k)+r\left\{b_k\Delta u(\mathbf{x},t_1)+\sum_{j=0}^{k-1}b_j\left[\Delta u(\mathbf{x},t_{k+1-j})-\Delta u(\mathbf{x},t_{k-j})\right]\right\}\\ &\quad+\tfrac{\Delta t}{2}\left[f(u(\mathbf{x},t_{k+1}),\mathbf{x},t_{k+1})+f(u(\mathbf{x},t_k),\mathbf{x},t_k)\right]+R_{k+1}\end{aligned} \tag{11}$$

where $r=\kappa\frac{(\Delta t)^{\alpha}}{\Gamma(\alpha+1)}$, and

$$|R_{k+1}| \leq Cb_k(\Delta t)^{1+\alpha}. \tag{12}$$

The equation (11) can be rewritten as

$$\begin{aligned}&u(\mathbf{x},t_{k+1})-r\Delta u(\mathbf{x},t_{k+1})\\ &=u(\mathbf{x},t_k)+r\sum_{j=0}^{k-1}(b_{j+1}-b_j)\Delta u(\mathbf{x},t_{k-j})\\ &+\tfrac{\Delta t}{2}\left[f(u(\mathbf{x},t_{k+1}),\mathbf{x},t_{k+1})+f(u(\mathbf{x},t_k),\mathbf{x},t_k)\right]+R_{k+1}.\end{aligned} \tag{13}$$

Let $u^k = u^k(\mathbf{x})$ be the numerical approximation to $u(\mathbf{x},t_k)$, then the equation (1) can be discretized as the following scheme

$$\begin{aligned} u^{k+1} - r\Delta u^{k+1} &= u^k + r\sum_{j=0}^{k-1}(b_{j+1}-b_j)\Delta u^{k-j} \\ &\quad + \tfrac{\Delta t}{2}\left[f(u^{k+1},\mathbf{x},t_{k+1}) + f(u^k,\mathbf{x},t_k)\right], \quad k = 0,1,\ldots,K-1. \end{aligned} \tag{14}$$

$$u^0 = u_0(\mathbf{x}) \tag{15}$$

$$u^k|_{\partial\Omega} = g(\mathbf{x},t_k), \quad k = 0,1,\ldots,K. \tag{16}$$

2.2 Stability and Convergency

In order to discuss the stability and convergency of (14), let us introduce to the following inner product

$$(v,w) = \iint_{\Omega} v(\mathbf{x})w(\mathbf{x})dxdy \tag{17}$$

and norm in L^2

$$\|v\|_2 = [(v,v)]^{1/2} = \left[\iint_{\Omega} v^2(\mathbf{x})dxdy\right]^{1/2} \tag{18}$$

Suppose that $\widetilde{u}^k = \widetilde{u}^k(\mathbf{x})$, $k = 1,2,\ldots,n$ is the solution of the Eq. (14) with the initial condition $u(\mathbf{x},0) = \widetilde{u}^0$ and the boundary condition (16), then the error $\varepsilon^k(\mathbf{x}) = u^k(\mathbf{x}) - \widetilde{u}^k(\mathbf{x})$ satisfies

$$\begin{aligned} \varepsilon^{k+1} - r\Delta\varepsilon^{k+1} &= \varepsilon^k + r\sum_{j=0}^{k-1}(b_{j+1}-b_j)\Delta\varepsilon^{k-j} \\ &\quad + \tfrac{\Delta t}{2}\left[f(u^{k+1},\mathbf{x},t_{k+1}) - f(\widetilde{u}^{k+1},\mathbf{x},t_{k+1})\right] \\ &\quad + \tfrac{\Delta t}{2}\left[f(u^k,\mathbf{x},t_k) - f(\widetilde{u}^k,\mathbf{x},t_k)\right], \end{aligned} \tag{19}$$

$$\varepsilon^0 = u(\mathbf{x},0) - \widetilde{u}^0(\mathbf{x}), \tag{20}$$

$$\varepsilon^{k+1}|_{\partial\Omega} = 0. \tag{21}$$

Theorem 1 The fractional implicit numerical method defined by (14) is un-conditionally stable. And we have

$$\|\varepsilon^k\|_2 \le e^{LT}\|\varepsilon^0\|_2.$$

Proof Multiplying (19) by ε^{k+1} and integrating on Ω, we obtain

$$\begin{aligned}
&(\varepsilon^{k+1},\varepsilon^{k+1})-r(\Delta\varepsilon^{k+1},\varepsilon^{k+1})\\
&=(\varepsilon^{k},\varepsilon^{k+1})+r\sum_{j=0}^{k-1}(b_{j+1}-b_j)(\Delta\varepsilon^{k-j},\varepsilon^{k+1})\\
&+\tfrac{\Delta t}{2}\left(f(u^{k+1},\mathbf{x},t_{k+1})-f(\widetilde{u}^{k+1},\mathbf{x},t_{k+1}),\varepsilon^{k+1}\right)\\
&+\tfrac{\Delta t}{2}\left(f(u^{k},\mathbf{x},t_{k})-f(\widetilde{u}^{k},\mathbf{x},t_{k}),\varepsilon^{k+1}\right),
\end{aligned}\tag{22}$$

i. e.,

$$\begin{aligned}
&\|\varepsilon^{k+1}\|_2^2+r\left(\|\tfrac{\partial\varepsilon^{k+1}}{\partial x}\|_2^2+\|\tfrac{\partial\varepsilon^{k+1}}{\partial y}\|_2^2\right)\\
&=(\varepsilon^{k},\varepsilon^{k+1})+r\sum_{j=0}^{k-1}(b_j-b_{j+1})\left[\left(\tfrac{\partial\varepsilon^{k-j}}{\partial x},\tfrac{\partial\varepsilon^{k+1}}{\partial x}\right)+\left(\tfrac{\partial\varepsilon^{k-j}}{\partial y},\tfrac{\partial\varepsilon^{k+1}}{\partial y}\right)\right]\\
&+\tfrac{\Delta t}{2}\left(f(u^{k+1},\mathbf{x},t_{k+1})-f(\widetilde{u}^{k+1},\mathbf{x},t_{k+1}),\varepsilon^{k+1}\right)\\
&+\tfrac{\Delta t}{2}\left(f(u^{k},\mathbf{x},t_{k})-f(\widetilde{u}^{k},\mathbf{x},t_{k}),\varepsilon^{k+1}\right),
\end{aligned}\tag{23}$$

Using Schwarz inequality, from (4) and the inequality[Liu, Zhuang, Anh, Turner, and Burrage (2007)]

$$b_j\geq b_{j+1},\ j=0,1,\ldots,K-1,$$

we have

$$\begin{aligned}
&\|\varepsilon^{k+1}\|_2^2+r\left(\|\tfrac{\partial\varepsilon^{k+1}}{\partial x}\|_2^2+\|\tfrac{\partial\varepsilon^{k+1}}{\partial y}\|_2^2\right)\\
&\leq\tfrac{1}{2}\left[\|\varepsilon^{k}\|_2^2+\|\varepsilon^{k+1}\|_2^2\right]\\
&+\tfrac{r}{2}\sum_{j=0}^{k-1}(b_j-b_{j+1})\left[\|\tfrac{\partial\varepsilon^{k-j}}{\partial x}\|_2^2+\|\tfrac{\partial\varepsilon^{k-j}}{\partial y}\|_2^2+\|\tfrac{\partial\varepsilon^{k+1}}{\partial x}\|_2^2+\|\tfrac{\partial\varepsilon^{k+1}}{\partial y}\|_2^2\right]\\
&+\tfrac{\Delta tL}{2}\|\varepsilon^{k+1}\|_2^2+\tfrac{\Delta tL}{2}\cdot\tfrac{1}{2}\left[\|\varepsilon^{k}\|_2^2+\|\varepsilon^{k+1}\|_2^2\right],
\end{aligned}\tag{24}$$

Note that $\sum_{j=0}^{k-1}(b_j-b_{j+1})=1-b_k\leq 1$, hence,

$$\begin{aligned}
&(1-\tfrac{3}{2}\Delta tL)\|\varepsilon^{k+1}\|_2^2+r\sum_{j=0}^{k}b_j\left[\|\tfrac{\partial\varepsilon^{k+1-j}}{\partial x}\|_2^2+\|\tfrac{\partial\varepsilon^{k+1-j}}{\partial y}\|_2^2\right]\\
&\leq\|\varepsilon^{k}\|_2^2+r\sum_{j=0}^{k-1}b_j\left[\|\tfrac{\partial\varepsilon^{k-j}}{\partial x}\|_2^2+\|\tfrac{\partial\varepsilon^{k-j}}{\partial y}\|_2^2\right]+\tfrac{1}{2}\Delta tL\|\varepsilon^{k}\|_2^2,
\end{aligned}\tag{25}$$

Let $E_k=\|\varepsilon^{k}\|_2^2+r\sum_{j=0}^{k-1}b_j\left[\|\tfrac{\partial\varepsilon^{k-j}}{\partial x}\|_2^2+\|\tfrac{\partial\varepsilon^{k-j}}{\partial y}\|_2^2\right]$, then

$$(1-\frac{3}{2}\Delta tL)E_{k+1}\leq(1+\frac{1}{2}\Delta tL)E_k$$

i. e.,

$$E_{k+1} \leq \frac{1+\frac{1}{2}\Delta tL}{1-\frac{3}{2}\Delta tL}E_k \leq \left(\frac{1+\frac{1}{2}\Delta tL}{1-\frac{3}{2}\Delta tL}\right)^2 E_{k-1} \leq \ldots \leq \left(\frac{1+\frac{1}{2}\Delta tL}{1-\frac{3}{2}\Delta tL}\right)^{k+1} E_0.$$

Hence, for $\forall\ 1 \leq k \leq n$, we have

$$\|\varepsilon^k\|_2^2 \leq E_k \leq \left(\frac{1+\frac{1}{2}\Delta tL}{1-\frac{3}{2}\Delta tL}\right)^K E_0 \leq \left(\frac{1+\frac{LT}{2K}}{1-\frac{3LT}{2K}}\right)^K E_0 \leq e^{2LT}\|\varepsilon^0\|_2^2.$$

Theorem 2 Suppose that the exact solution $u(\mathbf{x},t)$ of (1)-(3) satisfies $\frac{\partial^2 u(\mathbf{x},t)}{\partial t^2} \in C(\Omega \times [0,T])$, $\left\{u^k(\mathbf{x})\right\}_{k=0}^K$ be the time-discrete solution of (14) with initial condition $u^0(\mathbf{x}) = u(\mathbf{x},0)$ and the boundary condition (16), then we have the following error estimates

$$\|u(\mathbf{x},t_k) - u^k(\mathbf{x})\|_2 \leq C\Delta t, \tag{26}$$

where C is a positive constant.

Proof Let $\xi^k(\mathbf{x}) = u(\mathbf{x},t_k) - u^k(\mathbf{x})$, from (11) and (14), we obtain

$$\begin{aligned} \xi^{k+1} - r\Delta\xi^{k+1} &= \xi^k + r\sum_{j=0}^{k-1}(b_{j+1}-b_j)\Delta\xi^{k-j} \\ &\quad + \tfrac{\Delta t}{2}\left[f(u(\mathbf{x},t_{k+1}),\mathbf{x},t_{k+1}) - f(u^{k+1},\mathbf{x},t_{k+1})\right] \\ &\quad + \tfrac{\Delta t}{2}\left[f(u(\mathbf{x},t_k),\mathbf{x},t_k) - f(u^k,\mathbf{x},t_k)\right] + R_{k+1}, \end{aligned} \tag{27}$$

$$\xi^0(\mathbf{x}) = 0, \tag{28}$$

$$\xi^k(\mathbf{x})|_{\partial\Omega} = 0. \tag{29}$$

where $R_{k+1} \leq Cb_k(\Delta t)^{1+\alpha}$.

Multiplying (19) by ξ^{k+1} and integrating on Ω, we obtain

$$\begin{aligned} &\|\xi^{k+1}\|_2^2 + r\left(\|\tfrac{\partial\xi^{k+1}}{\partial x}\|_2^2 + \|\tfrac{\partial\xi^{k+1}}{\partial y}\|_2^2\right) \\ &= (\xi^k,\xi^{k+1}) + r\sum_{j=0}^{k-1}(b_j - b_{j+1})\left[\left(\tfrac{\partial\xi^{k-j}}{\partial x},\tfrac{\partial\xi^{k+1}}{\partial x}\right) + \left(\tfrac{\partial\xi^{k-j}}{\partial y},\tfrac{\partial\xi^{k+1}}{\partial y}\right)\right] \\ &+ \tfrac{\Delta t}{2}\left(f(u(\mathbf{x},t_{k+1}),\mathbf{x},t_{k+1}) - f(u^{k+1},\mathbf{x},t_{k+1}),\xi^{k+1}\right) \\ &+ \tfrac{\Delta t}{2}\left(f(u(\mathbf{x},t_k),\mathbf{x},t_k) - f(u^k,\mathbf{x},t_k),\xi^{k+1}\right) + (R_{k+1},\xi^{k+1}), \end{aligned} \tag{30}$$

Using Schwarz inequality, from (4) and the inequality[Liu, Zhuang, Anh, Turner, and Burrage (2007)]

$$b_j \geq b_{j+1},\ j = 0,1,\ldots,K-1,$$

we have

$$\begin{aligned}
&\|\xi^{k+1}\|_2^2 + r\left(\|\tfrac{\partial \xi^{k+1}}{\partial x}\|_2^2 + \|\tfrac{\partial \xi^{k+1}}{\partial y}\|_2^2\right) \\
&\le \tfrac{1}{2}\left[\|\xi^{k}\|_2^2 + \|\xi^{k+1}\|_2^2\right] \\
&+\tfrac{r}{2}\sum_{j=0}^{k-1}(b_j - b_{j+1})\left[\|\tfrac{\partial \xi^{k-j}}{\partial x}\|_2^2 + \|\tfrac{\partial \xi^{k-j}}{\partial y}\|_2^2 + \|\tfrac{\partial \xi^{k+1}}{\partial x}\|_2^2 + \|\tfrac{\partial \xi^{k+1}}{\partial y}\|_2^2\right] \\
&+\tfrac{3\Delta tL}{4}\|\xi^{k+1}\|_2^2 + \tfrac{\Delta tL}{4}\|\xi^{k}\|_2^2 + |(R_{k+1}, \xi^{k+1})|,
\end{aligned} \tag{31}$$

Note that $\sum_{j=0}^{k-1}(b_j - b_{j+1}) = 1 - b_k \le 1$, hence,

$$\begin{aligned}
&(1 - \tfrac{3}{2}\Delta tL)\|\xi^{k+1}\|_2^2 + r\sum_{j=0}^{k} b_j\left[\|\tfrac{\partial \xi^{k+1-j}}{\partial x}\|_2^2 + \|\tfrac{\partial \xi^{k+1-j}}{\partial y}\|_2^2\right] \\
&\le \|\xi^{k}\|_2^2 + r\sum_{j=0}^{k-1} b_j\left[\|\tfrac{\partial \xi^{k-j}}{\partial x}\|_2^2 + \|\tfrac{\partial \xi^{k-j}}{\partial y}\|_2^2\right] \\
&-b_k r\left[\|\tfrac{\partial \xi^{k+1}}{\partial x}\|_2^2 + \|\tfrac{\partial \xi^{k+1}}{\partial y}\|_2^2\right] + |(R_{k+1}, \xi^{k+1})| + \tfrac{1}{2}\Delta tL\|\xi^{k}\|_2^2,
\end{aligned} \tag{32}$$

Note that $\xi^k(\mathbf{x})|_{\partial\Omega} = 0$, using $\xi(x,y,t) = \int_a^x \frac{\partial \xi}{\partial x}dx = \int_a^y \frac{\partial \xi}{\partial y}dy$, we know that there is a positive constant A, such that

$$\|\xi^{k+1}\|_2^2 \le A\left[\|\frac{\partial \xi^{k+1}}{\partial x}\|_2^2 + \|\frac{\partial \xi^{k+1}}{\partial y}\|_2^2\right].$$

Thus,

$$\begin{aligned}
&(1 - \tfrac{3}{2}\Delta tL)\|\xi^{k+1}\|_2^2 + r\sum_{j=0}^{k} b_j\left[\|\tfrac{\partial \xi^{k+1-j}}{\partial x}\|_2^2 + \|\tfrac{\partial \xi^{k+1-j}}{\partial y}\|_2^2\right] \\
&\le (1 + \tfrac{1}{2}\Delta tL)\|\xi^{k}\|_2^2 + r\sum_{j=0}^{k-1} b_j\left[\|\tfrac{\partial \xi^{k-j}}{\partial x}\|_2^2 + \|\tfrac{\partial \xi^{k-j}}{\partial y}\|_2^2\right] - \tfrac{b_k r}{A}\|\xi^{k+1}\|_2^2 \\
&+|(R_{k+1}, \xi^{k+1})|,
\end{aligned} \tag{33}$$

Using $|(v,w)| \le a\|v\|_2^2 + \frac{1}{4a}\|w\|_2^2$ and

$$|(R_{k+1}, \xi^{k+1})| \le \frac{b_k r}{A}\|\xi^{k+1}\|_2^2 + \frac{A}{4b_k r}\|R_{k+1}\|_2^2 \le \frac{b_k r}{A}\|\xi^{k+1}\|_2^2 + Cb_k(\Delta t)^{2+\alpha}.$$

Let $\rho_k = \|\xi^k\|_2^2 + r\sum_{j=0}^{k-1} b_j\left[\|\frac{\partial \xi^{k-j}}{\partial x}\|_2^2 + \|\frac{\partial \xi^{k-j}}{\partial y}\|_2^2\right]$, then

$$\rho_{k+1} \le \frac{1 + \frac{1}{2}\Delta tL}{1 - \frac{3}{2}\Delta tL}\left[\rho_k + Cb_k(\Delta t)^{2+\alpha}\right].$$

i. e., for $\forall\ 1 \le k \le K$, we have

$$\|\xi^k\|_2^2 \le \rho_k \le \left(\frac{1+\frac{LT}{2K}}{1-\frac{3LT}{2K}}\right)^K \left[\rho_0 + C\sum_{j=0}^{K-1} b_k(\Delta t)^{2+\alpha}\right].$$

Note that $\sum_{j=0}^{K-1} b_k(\Delta t)^\alpha = (K\Delta t)^\alpha = T^\alpha$ and $\rho_0 = 0$, hence,

$$\|\xi^k\|_2^2 \le CT^\alpha e^{2LT}(\Delta t)^2,$$

i.e.,

$$\|\xi^k\|_2 \le \sqrt{CT^\alpha} e^{LT}\Delta t.$$

3 Meshless RBF shape functions

In this section, we present a collocation scheme using RBFs [Liu and Gu (2005); Song and Chen (2009)]to Eq. (14)-(16).

The approximation of a function $u(\mathbf{x})$, using RBF, may be written as a linear combination of n radial basis functions and m polynomial basis functions

$$u^h(\mathbf{x}) = \sum_{i=1}^{n} a_i R(\|\mathbf{r}-\mathbf{r}_i\|, c_i) + \sum_{j=1}^{m} a_{n+j} p_j(\mathbf{x}) \tag{34}$$

where $R(\|\mathbf{r}-\mathbf{r}_i\|, c_i)$ is the radial basis functions (RBF), n is the number of the nodes in the support domain of $\mathbf{x}$, $p_j(\mathbf{x})$ is monomials, m is the number of polynomial basis functions, coefficient a_i are interpolation coefficients. In the RBF $R(\|\mathbf{r}-\mathbf{r}_i\|, c_i)$, the variable is only the distance $\|\mathbf{r}-\mathbf{r}_i\|$, between the interpolation point $\mathbf{x}$ and a node $\mathbf{x}_i$.

There are a number of RBFs that can be used, such as

Modified Multi-quadrics(MQ) function

$$R(\|\mathbf{r}-\mathbf{r}_i\|, c_i) = \left(\|\mathbf{r}-\mathbf{r}_i\|^2 + c_i^2\right)^q,$$

Gaussian basis function

$$R(\|\mathbf{r}-\mathbf{r}_i\|, c_i) = e^{-c_i^2(\|\mathbf{r}-\mathbf{r}_i\|^2/r_c^2)},$$

and Thin plate spline function

$$R(\|\mathbf{r}-\mathbf{r}_i\|, c_i) = \|\mathbf{r}-\mathbf{r}_i\|^{2M}\log(\|\mathbf{r}-\mathbf{r}_i\|).$$

The MQ RBF replaces the classical finite difference and finite element spatial discretization schemes by a exponentially convergent, grid-free scattered data approximation scheme. Finite difference and finite element methods use low-order polynomial basis functions. MQ in contrast is very high order[Moridis and Kansa (1994)]. The advantages/disadvantages associated with finite difference, finite element, and MQ methods have been widely discussed. In this paper, we apply the MQ scheme to solve the two-dimensional anomalous subdiffusion equation with nolinear source term.

The second term of Eq. (34) consists of polynomials. To ensure invertible interpolation matrix of RBF, the polynomial is often needed to augment RBF to guarantee the non-singularity of the Matrix. In addition, the linear polynomial added into the RBF can also ensure linear consistence and improve the interpolation accuracy. In this study, we take linear polynomial, i. e., $m = 3$.

The cofficients a_i in equation (34) can be determined by enforcing that the function interpolations pass through all n nodes within the support domain. To square the system of equations, an extra m equations are required. This is ensured by the m conditions for (34), viz,

$$\sum_{j=1}^{n_i} a_j^{(i)} p_l^{(i)}(\mathbf{x}_j) = 0, \;\; l = 1,\ldots,m \tag{35}$$

In this paper, the interpolations of a function at the $k^{\mathtt{th}}$ point can have the form of

$$\widehat{u}(\mathbf{x}_k) = \sum_{i=1}^{n} a_i R(\|\mathbf{r}_k - \mathbf{r}_i\|, c_i) + a_{n+1}x_k + a_{n+2}y_k + a_{n+3}, \;\; k = 1,2,\ldots,n. \tag{36}$$

The function interpolation can be expressed in a matrix form as follows:

$$\widehat{\mathbf{u}}^e = G\mathbf{a}, \tag{37}$$

$$\mathbf{G} = \begin{pmatrix} R(\|\mathbf{r}_1 - \mathbf{r}_1\|, c_i) & \cdots & R(\|\mathbf{r}_1 - \mathbf{r}_n\|, c_i) & x_1 & y_1 & 1 \\ \vdots & \ddots & \vdots & \vdots & \vdots & \vdots \\ R(\|\mathbf{r}_n - \mathbf{r}_1\|, c_i) & \cdots & R(\|\mathbf{r}_n - \mathbf{r}_n\|, c_i) & x_n & y_n & 1 \\ x_1 & \cdots & x_n & 0 & 0 & 0 \\ y_1 & \cdots & y_n & 0 & 0 & 0 \\ 1 & \cdots & 1 & 0 & 0 & 0 \end{pmatrix} \tag{38}$$

$$\widehat{\mathbf{u}}^e = [\widehat{u}(\mathbf{x}_1),\ldots,\widehat{u}(\mathbf{x}_n),0,0,0]^{\mathtt{T}}, \tag{39}$$

$$\mathbf{a} = [a_1,\ldots,a_n,a_{n+1},a_{n+2},a_{n+3}]^{\mathtt{T}}, \tag{40}$$

Thus, the known coefficients vector is found to be

$$\mathbf{a} = \mathbf{G}^{-1}\widehat{\mathbf{u}}^e. \tag{41}$$

The form of the approximation function can be obtained as follows:

$$\widehat{u}(\mathbf{x}) = \varphi\mathbf{a} = \varphi\mathbf{G}^{-1}\widehat{\mathbf{u}}^e = \psi\widehat{\mathbf{u}}^e \tag{42}$$

$$\varphi = [R(\|\mathbf{r}-\mathbf{r}_1\|,c_1), R(\|\mathbf{r}-\mathbf{r}_2\|,c_2), \ldots, R(\|\mathbf{r}-\mathbf{r}_n\|,c_n), x, y, 1]_{1\times n} \tag{43}$$

where the matrix of shape functions can be expressed as follows

$$\psi = \varphi\mathbf{G}^{-1} = [\psi_1, \psi_2, \ldots, \psi_n, \psi_{n+1}, \Psi_{n+2}, \Psi_{n+3}]_{1\times n+3} \tag{44}$$

in which $\psi_i (i = 1,2,\ldots,n)$ are shape functions for points in the support domain, which satisfy

$$\psi_i(\mathbf{x}_j) = \begin{cases} 1, & j = i \\ 0, & j \neq i. \end{cases} \tag{45}$$

Thus, the function $u(\mathbf{x})$ can be expressed as follows

$$u(\mathbf{x}) = \sum_{k=1}^{n} \psi_k \widehat{u}_k^e. \tag{46}$$

4 Meshless Scheme

In this section, we give the meshless scheme of the problem (14)-(16).

Assume that there are N_d internal (domain) points $\mathbf{x}_1, \mathbf{x}_2, \ldots, \mathbf{x}_{N_d}$ and N_b boundary points $\mathbf{x}_{N_b+1}, \mathbf{x}_{N_b+2}, \ldots, \mathbf{x}_{N_d+N_b}$. For $i = 1,2,\ldots,N_d$, we suppose that $\mathbf{x}_{i_1}, \mathbf{x}_{i_2}, \ldots, \mathbf{x}_{i_{n_i}}$ are the nodes in the support domain S_i of $\mathbf{x}_i$.

From (14), the following N_d equations are satisfied at internal domain nodes

$$\begin{aligned} \widehat{u}_i^{k+1} - r\Delta\widehat{u}_i^{k+1} &= \widehat{u}_i^k + r\sum_{j=0}^{k-1}(b_{j+1}-b_j)\Delta\widehat{u}_i^{k-j} \\ &\quad +0.5\Delta t\left[f(\widehat{u}_i^{k+1}, \mathbf{x}_i, t_{k+1}) + f(\widehat{u}_i^k, \mathbf{x}_i, t_k)\right], \quad i = 1,2,\ldots,N_d. \end{aligned} \tag{47}$$

The following N_b equations are satisfied on $\partial\Omega$

$$\widehat{u}_i^{k+1} = g(\mathbf{x}_i, t_{k+1}), \quad i = N_d+1, N_d+2, \ldots, N_d+N_b. \tag{48}$$

Let $D_i = \{i_1, i_2, \ldots, i_{n_i}\}$. Using the meshless shape functions, for $\mathbf{x} \in S_i$, $\widehat{u}_i^{k+1}$ can be written as

$$\widehat{u}^{k+1}(\mathbf{x}) = \sum_{j \in D_i} \psi_j^{(i)}(\mathbf{x}) \widehat{u}_j^{k+1,e}, \tag{49}$$

and the derivatives can be written as

$$\begin{aligned} \frac{\partial \widehat{u}^{k+1}(\mathbf{x})}{\partial x} &= \sum_{j \in D_i} \frac{\partial \Psi_j^{(i)}}{\partial x} \widehat{u}_j^{k+1,e}, \quad \frac{\partial^2 \widehat{u}^{k+1}(\mathbf{x})}{\partial x^2} = \sum_{j \in D_i} \frac{\partial^2 \Psi_j^{(i)}}{\partial x^2} \widehat{u}_j^{k+1,e}, \\ \frac{\partial \widehat{u}^{k+1}(\mathbf{x})}{\partial y} &= \sum_{j \in D_i} \frac{\partial \Psi_j^{(i)}}{\partial y} \widehat{u}_j^{k+1,e}, \quad \frac{\partial^2 \widehat{u}^{k+1}(\mathbf{x})}{\partial y^2} = \sum_{j \in D_i} \frac{\partial^2 \Psi_j^{(i)}}{\partial y^2} \widehat{u}_j^{k+1,e}. \end{aligned} \tag{50}$$

Substituting into (14), then for $i = 1, 2, \ldots, N_d$,

$$\begin{aligned} &\sum_{j \in D_i} \left[\Psi_j^{(i)}(\mathbf{x}_i) - r \Delta \Psi_j^{(i)}(\mathbf{x}_i) \right] \widehat{u}_j^{k+1,e} \\ &= \sum_{j \in D_i} \psi_j^{(i)}(\mathbf{x}_i) \widehat{u}_j^{k,e} + r \sum_{l=0}^{k-1} (b_{l+1} - b_l) \sum_{j \in D_i} \Delta \psi_j^{(i)}(\mathbf{x}_i) \widehat{u}_j^{k-l,e} \\ &+ 0.5 \Delta t \left[f\Big(\sum_{j \in D_i} \Psi_j^{(i)}(\mathbf{x}_i) \widehat{u}_j^{k+1,e}, \mathbf{x}_i, t_{k+1} \Big) + f\Big(\sum_{j \in D_i} \Psi_j^{(i)}(\mathbf{x}_i) \widehat{u}_j^{k,e}, \mathbf{x}_i, t_k \Big) \right]. \end{aligned} \tag{51}$$

For $i = N_d + 1, N_d + 2, \ldots, N_d + N_b$,

$$\sum_{j \in D_i} \Psi_j^{(i)}(\mathbf{x}_i) \widehat{u}_i^{k+1,e} = g(\mathbf{x}_i, t_{k+1}), \tag{52}$$

or

$$\widehat{u}_i^{k+1,e} = g(\mathbf{x}_i, t_{k+1}). \tag{53}$$

Thus, $\widehat{u}_i^{k+1}$ and its derivatives can be obtain by substituting $\mathbf{x}$ into $\mathbf{x}_i$ in equations (49) and (50)

$$\begin{aligned} &\widehat{u}_i^{k+1} = \widehat{u}^{k+1}(\mathbf{x}_i), \quad \frac{\partial \widehat{u}_i^{k+1}}{\partial x} = \frac{\partial \widehat{u}^{k+1}(\mathbf{x}_i)}{\partial x}, \quad \frac{\partial \widehat{u}_i^{k+1}}{\partial y} = \frac{\partial \widehat{u}^{k+1}(\mathbf{x}_i)}{\partial y}, \\ &\frac{\partial^2 \widehat{u}_i^{k+1}}{\partial x^2} = \frac{\partial^2 \widehat{u}^{k+1}(\mathbf{x}_i)}{\partial x^2}, \quad \frac{\partial^2 \widehat{u}_i^{k+1}}{\partial y^2} = \frac{\partial^2 \widehat{u}^{k+1}(\mathbf{x}_i)}{\partial y^2}. \end{aligned} \tag{54}$$

5 Test Examples

In this section, we present some numerical examples to demonstrate the effectiveness of the newly algorithm. In all presented examples, we have used the multiquadric(MQ) RBF function as

$$R_i(r) = (r_i^2 + (\alpha_c d_c)^2)^q$$

where $\alpha_c = 2.0$, $q = 1.03$ and d_c is a characteristic length that is related to the nodal spacing in the local domain of the point of interest.

To investigate the accuracy and efficiency, we introduce the following error notations

$$\begin{aligned} &\varepsilon_{\max} = \max_i |u_i^{\mathtt{exact}} - u_i^{\mathtt{num}}|, \quad \varepsilon_0 = \sqrt{\frac{\sum_{i=1}^{N_d} (u_i^{\mathtt{exact}} - u_i^{\mathtt{num}})^2}{\sum_{i=1}^{N_d} (u_i^{\mathtt{exact}})^2}} \\ &\varepsilon_x = \sqrt{\frac{\sum_{i=1}^{N_d} (u_{i,x}^{\mathtt{exact}} - u_{i,x}^{\mathtt{num}})^2}{\sum_{i=1}^{N_d} (u_{i,x}^{\mathtt{exact}})^2}}, \quad \varepsilon_y = \sqrt{\frac{\sum_{i=1}^{N_d} (u_{i,y}^{\mathtt{exact}} - u_{i,y}^{\mathtt{num}})^2}{\sum_{i=1}^{N_d} (u_{i,y}^{\mathtt{exact}})^2}} \end{aligned} \tag{55}$$

and the error function $\varepsilon(x,y,t) = |u^{\mathtt{exact}}(x,y,t) - u^{\mathtt{num}}(x,y,t)|$.

In which $\varepsilon_0, \varepsilon_x$ and ε_y are the error norms for the solution and its derivatives with respect to x and y, respectively, $u_i^{\mathtt{exact}}$ and $u_i^{\mathtt{num}}$ are the exact and the numerical solutions at node i, respectively, $u_{i,x}$ and $u_{i,y}$ are derivatives of the solution with respect to x and y, respectively, and N_d is the internal (domain) points.

5.1 Anomalous subdiffusion equation with linear source term

As a test equation, we consider the following anomalous subdiffusion equation with linear source term

$$\frac{\partial u}{\partial t} =_0 D_t^{1-\alpha} \Delta u(\mathbf{x},t) + f(\mathbf{x},t), \quad x \in \Omega \subset \mathbf{R}^2, \quad t > 0 \tag{56}$$

together with the general boundary condition

$$u(\mathbf{x},t) = t^{2+\alpha} e^{x+y}, \quad \mathbf{x} \in \quad \partial\Omega, \quad t > 0 \tag{57}$$

and initial condition

$$u(\mathbf{x},0) = 0 \tag{58}$$

where $f(\mathbf{x},t) = \left[(2+\alpha) t^{1+\alpha} - \frac{2\Gamma(3+\alpha)}{\Gamma(2+2\alpha)} t^{1+2\alpha} \right] e^{x+y}$.

The exact solution of (56)-(58) is $u(x,y,t) = t^{2+\alpha} e^{x+y}$.

Firstly, the problem domain is considered with $\Omega = [0,1] \times [0,1]$. We choose $n = 21 \times 21$ collocation points all together. The nodes distribution is shown in Fig. 1. The proposed method is used to simulate this problem, Fig. 2 plots the computational errors for different time steps. It has been found, the error reduces with the descrease of time steps.

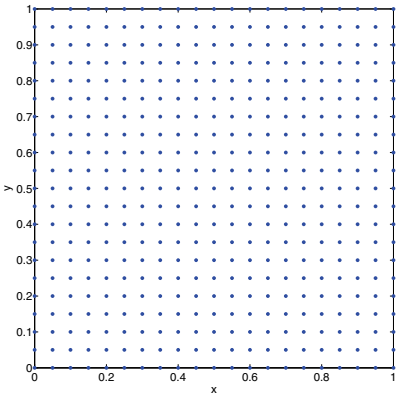

Figure 1: Regular nodal distribution for rectangular domain

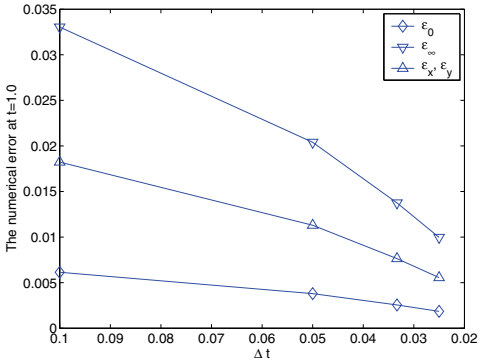

Figure 2: Errors as a function of the time step Δt(Regular nodal distribution shown in Fig. 1 is used)

Secondly, the irregularly distributed nodes are also used, as shown in Fig. 3. The computational errors for different time steps are plotted in Fig. 4. Similar as the results presented in Fig. 2, the computational errors in Fig. 4 also decrease with time steps. In other words, a small time step leads to a more accurate result. The influences of different α are also studied. Figs. 5, 6 and 7 plot the computational errors for $\alpha = 0.5$, 0.7 and 0.9, respectively. The maximum errors for these three different α are in the similar order of 10^{-3}. The above figures have proven that the newly proposed meshless approach has very good accuracy and convergence even using irregular nodal distributions. It should mention here that the irregular grid will lead to a big difficulty for the conventional FDM.

A circular problem domain with $\Omega = \left\{(x,y)\,\middle|\, x^2+y^2 \le 1\right\}$ is also considered, and the irregular nodal distribution is employed as shown in Fig. 8. The computational errors for different time steps are plotted in Fig. 9. The presented meshless approach has led to a good convergence regarding to time steps. However, the conventional FDM is hard to handle this circular problem domain.

For comparison, the equation (58) with rectangular problem domain has been also simulated by the conventional FDM based on the regular grid. It has been found the proposed meshless approach leads to more accurate results than FDM when their computational errors are in the same order.

In summary, the above investigations have proven that the newly proposed meshless method is accurate, convergent and effective for the ASDE discussed. It should be mentioned that the present approach is robust for irregular nodal distributions and different problem domains including non-rectangular problem domains, which conventional FDM is difficult to handle.

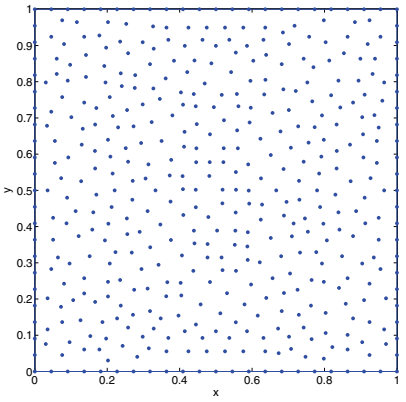

Figure 3: Irregular nodal distribution for the rectangular domain

5.2 Anomalous subdiffusion equation with nonlinear source term

We consider the following anomalous subdiffusion equation with nonlinear source term

$$\frac{\partial u}{\partial t} =_0 D_t^{1-\alpha}\Delta u(\mathbf{x},t) - u^2 + f(\mathbf{x},t),\ \ x \in \Omega \subset \mathbf{R}^2,\ \ t > 0 \tag{59}$$

together with the general boundry condition

$$u(\mathbf{x},t) = t^{2+\alpha}e^{x+y},\ \ \mathbf{x} \in\ \ \partial\Omega,\ \ t > 0 \tag{60}$$

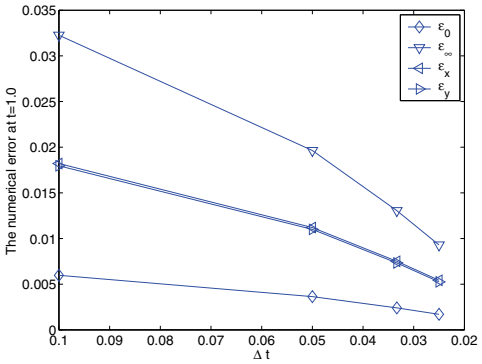

Figure 4: Errors as a function of the time step Δt(Irregular nodal distribution shown in Fig. 3 is used)

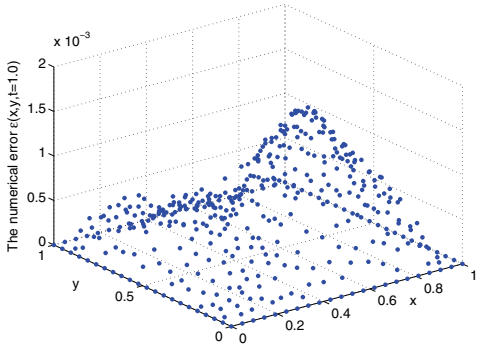

Figure 5: The error distribution for $\alpha = 0.5$ at $t = 1.0$

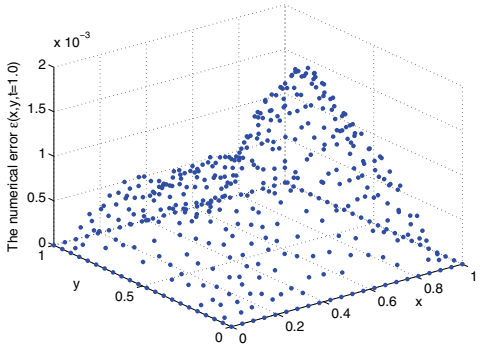

Figure 6: The error distribution for $\alpha = 0.7$ at $t = 1.0$

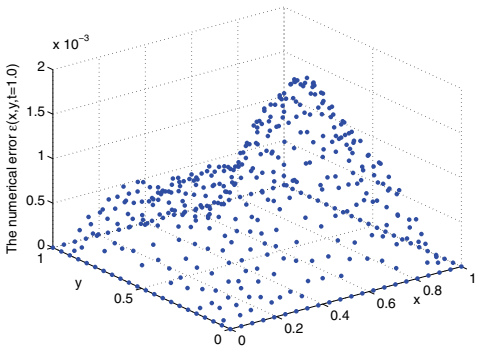

Figure 7: The error distribution for $\alpha = 0.9$ at $t = 1.0$

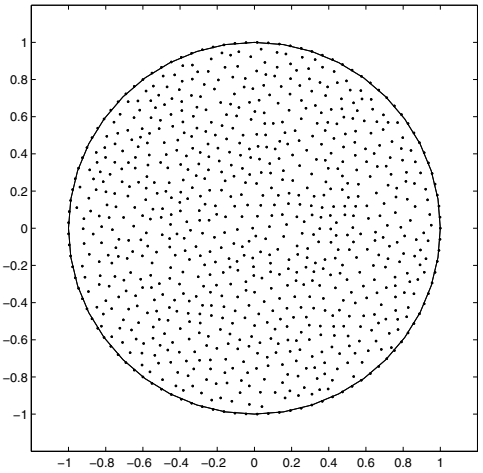

Figure 8: Irregular nodal distribution for the circular domain

and initial condition

$$u(\mathbf{x},0) = 0 \tag{61}$$

where $f(\mathbf{x},t) = \left[(2+\alpha)t^{1+\alpha} - \frac{2\Gamma(3+\alpha)}{\Gamma(2+2\alpha)}t^{1+2\alpha} + t^{2+4\alpha}e^{x+y}\right]e^{x+y}$.

The exact solution of (59)-(61) is $u(x,y,t) = t^{2+\alpha}e^{x+y}$.

To simulate this nonlinear ASDE, similar to the Example 5.1, the rectangular problem domain, as shown in Fig. 1, and both regular and irregular nodal distributions, as shown in Fig. 1 and Fig. 3, are considered. The convergence processes regarding to time steps are plotted in Fig. 10 and Fig. 11, respectively. It can be found that both regular and irregular nodal distributions lead to good convergence for nonlin-

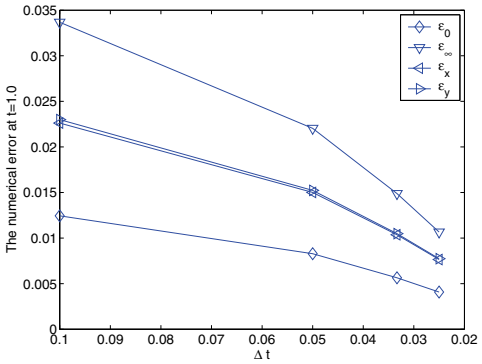

Figure 9: Errors as a function of the time step Δt(Irregular nodal distribution shown in Fig. 8 is used)

ear ASDE. The circular problem domain with irregular nodal distribution, as shown in Fig. 8, is also considered. The computational errors for different time steps for this circular problem domain governed by the nonlinear ASDE has been obtained as plotted in Fig. 12. The distributions of computational errors for different cases of α are presented in Figs. 13, 14 and 15. Very good accuracy and convergence have been obtained.

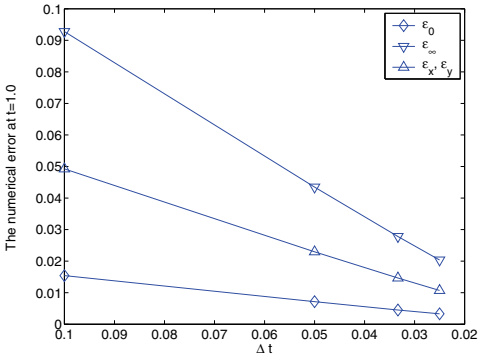

Figure 10: Computational errors for the nonlinear ASDE(Regular nodal distribution shown in Fig. 1 is used)

5.3 Anomalous subdiffusion equation with a Fisher nonlinear source term

Fisher[Fisher (1937)] proposed a reaction diffusion equation as a model to describe the process of spatial spreading when mutant individuals with higher adaptability

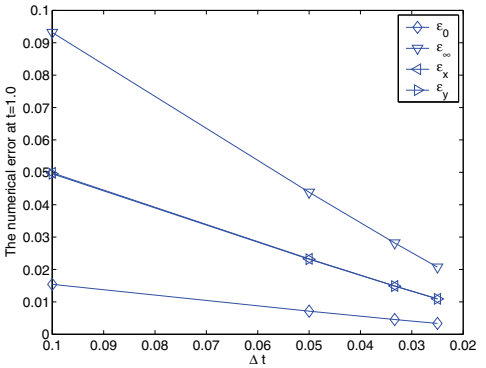

Figure 11: Errors as a function of the time step Δt(Irregular distribution shown in fig. 3 is used)

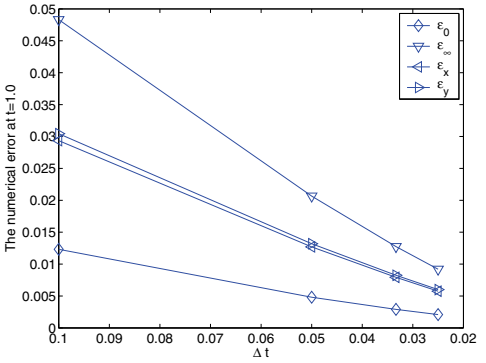

Figure 12: Errors as a function of the time step Δt(Irregular nodal distribution shown in fig. 8 is used)

appear in populations, namely

$$u_t = \Delta u + (1-u)u \tag{62}$$

This equation is well known in the field of population genetics. On the other hand, in the field of theoretical ecology, Skellam [Skellam (1951)] used the following diffusion equation to explain spatial patterns of biological individuals,

$$u_t = \kappa \Delta u + \mu(1-u/B)u \tag{63}$$

where $\mu > 0$ is the intrinsic growth rate, $B > 0$ is the carrying capacity and u is the density of a biological population.

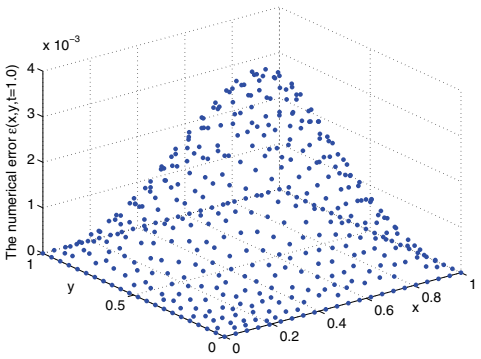

Figure 13: The error distribution for $\alpha = 0.5$ at $t = 1.0$

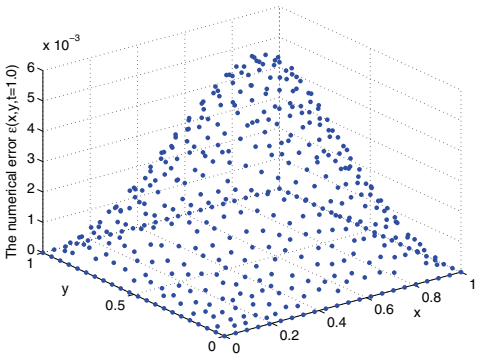

Figure 14: The error distribution for $\alpha = 0.7$ at $t = 1.0$

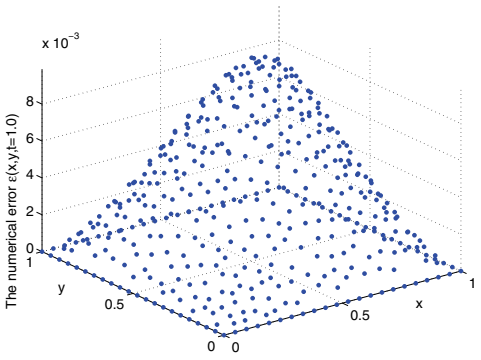

Figure 15: The error distribution for $\alpha = 0.9$ at $t = 1.0$

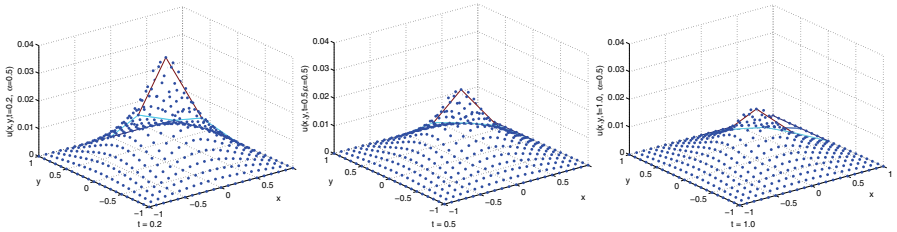

Figure 16: The numerical solution For Eq.(46)-(48) where $\alpha = 0.5$

Let's consider the following anomalous subdiffusion equation with a Fisher nonlinear source termn[Lynch, Carreras, del Castillo-Negrete, Ferreira-Mejias, and Hicks (2003)]

$$\frac{\partial u}{\partial t} = \kappa_\alpha \cdot D_0^{1-\alpha} \Delta u + \mu u(1-u/B), \tag{64}$$

$$u(\mathbf{x},t) = 0, \ \ \mathbf{x} \in \ \partial\Omega, \ \ t > 0 \tag{65}$$

$$u(\mathbf{x},0) = 10 \max\left\{0.8, e^{-100(x^2+y^2)}\right\}, (x,y) \in \Omega. \tag{66}$$

where $\Omega = [0,1] \times [0,1]$. In this example, we take $\alpha = 0.5$, $\kappa_\alpha = 1.0$, $\mu = 0.5$, $B = 1.0$.

It should be mentioned here that there is no exact solution for this problem. Instead, as a reference solution, we simulated this problem by FDM using very fine regular grids.

The rectangular problem domain discretized by regular distributed nodes (as shown in Fig. 1) is considered. Taking $\Delta t = 10^{-3}$, Fig. 16-18 show distributions of u numerically obtained by the newly proposed meshless approach for different α when $t = 0.2,\ 0.5,\ 1.0$, respectively. From these figures, we can find that the wave travels more slowly as α decreases. This shows a same tendency as its natural properties.

The conventional FDM based on the regular grid is also used to simulate this problem. It has been found that, even using the irregular nodal distribution, the present approach leads to more accurate results than FDM (using the regular grids).

6 Conclusion

This paper has proposed an implicit meshless approach based on the radial basis functions for numerical simulation of the non-linear anomalous subdiffusion equation , which is a type of fractional partial differential equation. The discrete system

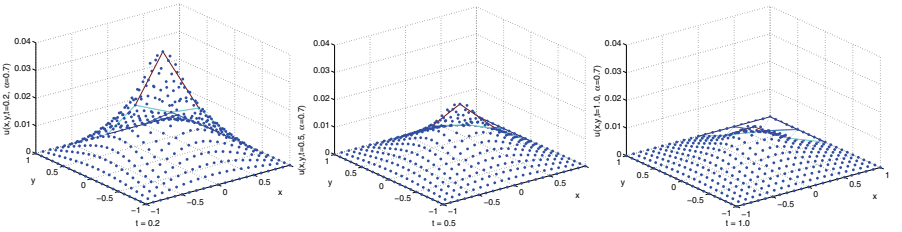

Figure 17: The numerical solution For Eq.(46)-(48) where $\alpha = 0.7$

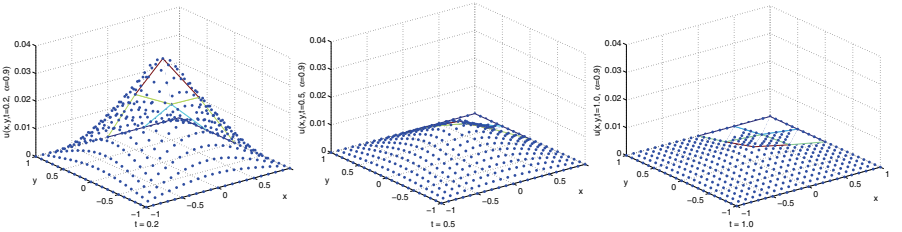

Figure 18: The numerical solution For Eq.(46)-(48) where $\alpha = 0.9$

of equations is obtained by using the meshless shape functions and the strong-forms. The stability and convergence of this meshless approach are then discussed and theoretically proven. Several numerical examples with different problem domains are used to validate and investigate accuracy and efficiency of the newly developed meshless formulation. The results obtained by the meshless formulations are also compared with those obtained by FDM in terms of their accuracy and efficiency.

The following conclusions can be drawn through the studies in this paper.

- The present implicit meshless formulation for time fractional differential equations is un-conditionally stable.
- The accuracy of this present numerical approach is with the order of Δt.
- If the same regular nodal distributions are used, the present meshless approach leads to more accurate results that FDM.
- The present meshless approach has good accuracy and convergence for irregular nodal distributions and complex problem domains.

In summary, the newly developed meshless approach is accurate and convergent. Most importantly, the present approach is robust for arbitrarily distributed nodes

and complex problem domains, for which the conventional FDM is difficult to handle. Hence, the present meshless formulation is very effective for the modelling and simulation of fractional differential equations, and it has good potential in development of a robust simulation tool for problems in engineering and science which are governed by the various types of fractional differential equations.

Acknowledgement: This work was supported by an ARC Discovery Grant.

References

Agrawal, O. P.; Machado, J. A. T.; Sabatier, J. (2004): Introduction. *Nonlinear Dynam.*, vol. 38, pp. 1–2.

Atluri, S.; Zhu, T. (1998a): A new meshless local Petrov-Galerkin (MLPG) approach in computational mechanics. *Computational Mechanics*, vol. 22, pp. 117–127.

Atluri, S. N.; Han, Z. D.; Rajendran, A. M. (2004): A New Implementation of the Meshless Finite Volume Method, Through the MLPG "Mixed" Approach. *CMES-Computer Modeling in Engineering and Sciences*, vol. 6(6), pp. 491–513.

Atluri, S. N.; Kim, H. G.; Cho, J. Y. (1999): A critical assessment of the truly meshless local Petrov-Galerkin (MLPG), and Local Boundary Integral Equation (LBIE) methods. *Computational Mechanics*, vol. 24, pp. 348–372.

Atluri, S. N.; Shen, S. P. (2002): *The Meshless Local Petrov-Galerkin (MLPG) method*. Tech Sciemce Press. Encino USA.

Atluri, S. N.; Shen, S. P. (2002): The meshless local Petrov-Galerkin (MLPG) method: A simple & less-costly alternative to the finite element and boundary element methods. *CMES-Computer Modeling in Engineering and Sciences*, vol. 3(1), pp. 11–51.

Atluri, S. N.; Zhu, T. (1998b): A new meshless local Petrov-Galerkin (MLPG) approach to nonlinear problems in computer modeling and simulation. *Computer Modeling and Simulation in Engineering*, vol. 3(3), pp. 187–196.

Belytschko, T.; Lu, Y. Y.; Gu, L. (1994): Element-free Galerkin methods. *Int. J. Numer. Methods Engrg.*, vol. 37, pp. 229–256.

Benson, D. A.; Wheatcraft, S. W.; Meerschaert, M. M. (2000): Application of a fractional advection¨Cdispersion equation. *Water Resour. Res.*, vol. 36(6), pp. 1403–1412.

Brown, E.; Wu, E.; Zipfel, W.; Webb, W. (1999): Measurement of molecular diffusion in solution by multiphoton fluorescence photobleaching recovery. *Biophys. J.*, vol. 77, pp. 2837–2849.

Butzer, P. L.; Georges, A. (2000): *An Introduction to Fractional Calculus*. World Scientific, Singapore.

Chechkin, A.; Gonchar, V. Y.; Kflafter, J.; Metzler, R. (2006): Fundamentals of Lévy flight processes. *Advances in Chemical Physics*, vol. 133, pp. 436–496.

Chen, C.-M.; Liu, F.; Turner, I.; Anh, V. (2007): Fourier method for the fractional diffusion equation describing sub-diffusion. *J. Comp. Phys.*, vol. 227, pp. 886–897.

Chen, W.; Ye, L.; Sun, H. (2010): Fractional diffusion equations by the Kansa method. *Computers and Mathematics with Applications.*, vol. 59(5), pp. 1614–1620.

Ching, H. K.; Batra, R. C. (2001): Determination of crack tip fields in linear elastostatics by the meshfree local Petrov-Galerkin (MLPG) method. *CMES-Computer Modeling in Engineering & Sciences*, vol. 12(2), pp. 273–289.

Ervin, V. J.; Heuer, N.; Roop, J. P. (2007): Numerical approximation of a time dependent, nonlinear, space-fractional diffusion equation. *SIAM J. Numer. Anal.*, vol. 45, pp. 572–591.

Ervin, V. J.; Roop, J. P. (2005): Variational formulation for the stationary fractional advection dispersion equation. *Numer. Methods Partial Differential Equations*, vol. 22, pp. 558–576.

Feder, T.; Brust-Mascher, I.; Slattery, J.; Baird, B.; Webb, W. (1996): Constrained diffusion or immobile fraction on cell surfaces: a new interpretation. *Biophys. J.*, vol. 70, pp. 2767–2773.

Fisher, R. A. (1937): The wave of advance of advantageous genes. *Ann. of Eugenics*, vol. 7, pp. 255–369.

Ghosh, R. (1991): Mobility and clustering of individual low density lipoprotein receptor molecules on the surface of human skin fibroblasts. *Ph.D. Thesis, Cornell University, Ithaca, NY.*

Ghosh, R.; Webb, W. (1994): Automated detection and tracking of individual and clustered cell surface low density lipoprotein receptor molecules. *Biophys. J.*, vol. 66, pp. 1301–1318.

Gingold, R. A.; Moraghan, J. (1977): Smooth particle hydrodynamics: theory and applications to non spherical stars. *Monthly Notices of the Royal Astronomical Society*, vol. 181, pp. 375–389.

Gu, Y.; Liu, G. (2001): A meshless Local Petrov-Galerkin (MLPG) formulation for static and free vibration analysis of thin plates. *CMES-Computer Modeling in Engineering & Sciences*, vol. 2(4), pp. 463–476.

Kansa, E. J. (1990): Multiquadrics-A Scattered Data Approximation Scheme with Applications to Computational Fluid dynamics. *Computers Math. Applic.*, vol. 19(8/9), pp. 127–145.

Kenneth, S. M.; Bertram, R. (1993): *An Introdution to the Fractional Calculus and Fractional Differential Equations*. Wiley-Interscience, New York.

Kou, C.; Yan, Y.; Liu, J. (2009): Stability Analysis for Fractional Differential Equations and Their Applications in the Models of HIV-1 Infection. *CMES-Computer Modeling in Engineering & Sciences*, vol. 39(3), pp. 301–318.

Langlands, T.; Henry, B. (2005): The accuracy and stability of an implicit solution method for the fractional diffusion equation. *J. Comput. Phys.*, vol. 205, pp. 719–736.

Le, P.; Mai-Duy, N.; Tran-Cong, T.; Baker, G. (2008): A meshless modeling of dynamic strain localization in quasi-brittle materials using radial basis function networks. *CMES-Computer Modeling in Engineering & Sciences*, vol. 25, pp. 43–66.

Li, S.; Atluri, S. N. (2008): The MLPG mixed collocation method for material orientation and topology optimization of anisotropic solids and structures. *CMES-Computer Modeling in Engineering & Sciences*, vol. 30(1), pp. 37–56.

Liu, F.; Zhuang, P.; Anh, V.; Turner, I.; Burrage, K. (2007): Stability and convergence of the difference methods for the space-time fractional advection-diffusion equation. *Applied Mathematics and Computation*, vol. 191, pp. 12–20.

Liu, G. R.; Gu, Y. T. (2005): *An introduction to meshfree methods and their programming*. Springer Press, Berlin.

Lynch, V. E.; Carreras, B. A.; del Castillo-Negrete, D.; Ferreira-Mejias, K. M.; Hicks, H. R. (2003): Numerical methods for the solution of partial differential equations of fractional order. *Journal of Computational Physics*, vol. 192, pp. 406–421.

Metzler, R.; Klafter, J. (2000): The random walk's guide to anomalous diffusion: a fractional dynamics approach. *Physics Reports*, vol. 339(1), pp. 1–77.

Metzler, R.; Klafter, J. (2004): The restaurant at the end of the random walk: recent developments in the description of anomalous transport by fractional dynamics. *Journal of Physics A: Mathematical and General*, vol. 37(2), pp. R161–R208.

Moridis, G.; Kansa, E. J. (1994): The Laplace transform multiquadric method highly accurate scheme for numerical solution of partial differential equations. *J. Appl. Sci. and Comput.*, vol. 1(2), pp. 375–407.

Nayroles, B.; Touzot, G.; Villon, P. (1992): Generalizing the finite element method: diffuse approximation and diffuse elements. *Computational Mechanics*, vol. 10, pp. 307–318.

Onate, E.; Idelsohn, S.; Zienkiewicz, O. C.; Taylor, R. L.; Sacco, C. (1996): A finite method in computational mechanics: applications to convective transport and fluid flow. *International Journal of Numerical Methods in Engineering*, vol. 39, pp. 3839–3866.

Saxton, M. (1994): Anomalous diffusion due to obstacles: a Monte Carlo Study. *Biophys. J.*, vol. 66, pp. 394–401.

Saxton, M. (1996): Anomalous diffusion due to binding: a Monte Carlo study. *Biophys. J.*, vol. 70, pp. 1250–1262.

Saxton, M. (2001): Anomalous subdiffusion in fluorescence photobleaching recovery: a Monte Carlo study. *Biophys. J.*, vol. 81, pp. 2226–2240.

Sheets, E.; Lee, G.; Simson, R.; Jacobson, K. (1997): Transient confinement of a glycosyl phosphatidylinositol-anchored protein in the plasma membrane. *Biochemistry*, vol. 36, pp. 12449–12458.

Simson, R.; Yang, B.; Moore, S.; Doherty, P.; Walsh, F.; Jacobson, K. (1998): Structural mosaicism on the submicron scale in the plasma membrane. *Biophys. J.*, vol. 74, pp. 297–308.

Skellam, J. (1951): Random dispersal in theoretical populations. *Biometrika*, vol. 38, pp. 196–218.

Slattery, J. (1991): Lateral mobility of FcRI on rat basophilic leukaemia cells as measured by single particle tracking using a novel bright fluorescent probe. *Ph.D. Thesis, Cornell University, Ithaca, NY*.

Smith, P.; Morrison, I.; Wilson, K.; Fernandez, N.; Cherry, R. (1999): Anomalous diffusion of major histocompatability complex class I molecules on HeLa cells determined by single particle tracking. *Biophys. J.*, vol. 76, pp. 3331–3344.

Sokolov, I.; Klafter, J. (2005): From diffusion to anomalous diffusion: a century after Einstein's brownian motion. *Chaos*, vol. 15, pp. 026103.

Sokolov, I.; Klafter, J.; Blumen, A. (2002): Fractional kinetic equations. *Physics Today*, vol. 55, pp. 48–54.

Song, R.; Chen, W. (2009): An investigation on the regularized meshless method for irregular domain problems. *CMES-Computer Modeling in Engineering & Sciences*, vol. 42(1), pp. 59–70.

Ye, H.; Ding, Y. (2009): Dynamical Analysis of a Fractional-order HIV Model. *CMES-Computer Modeling in Engineering & Sciences*, vol. 49(3), pp. 255–268.

Yuste, S. B.; Acedo, L. (2004): Some exact results for the trapping of subdiffusive particles in one dimension. *Phys. A*, vol. 336, pp. 334–346.

Yuste, S. B.; Acedo, L. (2005): An explicit finite difference method and a new von Neumann- type stability analysis for fractional diffusion equations. *SIAM J. Numer. Anal.*, vol. 42, pp. 1862–1874.

Zaslavsky, G. (2002): Chao, fractional kinetics, and anomalous transport. *Physics Reports*, vol. 371(1), pp. 461–580.

Zheng, J.; Long, S.; Xiong, Y.; Li, G. (2009): A Finite Volume Meshless Local Petrov-Galerkin Method for Topology Optimization Design of the Continuum Structures. *CMES-Computer Modeling in Engineering & Sciences*, vol. 42(1), pp. 19–34.

Zhu, T.; Atluri, S. N. (1998): A modified collocation method and a penalty formulationm for enforcing the essential boundary conditions in the element free Galerkin method. *Computational Mechanics*, vol. 21, pp. 211–222.

Zhuang, P.; Liu, F.; Anh, V.; Turner, I. (2008): New solution and analytical techniques of the implicit numerical method for the anomalous subdiffusion equation. *SIAM Journal on Numerical Analysis*, vol. 46(2), pp. 1079–1095.